J Therm Anal Calorim (2010) 100:423–429
DOI 10.1007/s10973-009-0645-8

Thermal analysis and crystallization from melts

β-adrenergic compounds

J. Canotilho · R. A. E. Castro · M. T. S. Rosado · S. C. C. Nunes · M. S. C. Cruz · J. S. Redinha

Portuguese Special Chapter
Received: 4 October 2008 / Accepted: 21 November 2009 / Published online: 21 January 2010

Abstract The growth of atenolol, pindolol and betaxolol hydrochloride from melt was investigated by differential scanning calorimetry (DSC) and polarized light thermal microscopy (PLTM). Phase transitions occurring on cooling and subsequent reheating runs performed between −160 °C and a temperature above the respective melting points were studied by DSC. The thermal cycles were also followed by PLTM. Details about the dynamic of the crystallization front taken from microscopic observations are given. An explanation of the results on the basis of molecular supramolecular recognition is advanced.

Keywords Thermal analysis · Growth from melt · Liquid immiscibility · Molecular recognition · β-Adrenergic compounds

Introduction

Melt growth techniques are widely used in industry for the preparation of inorganic crystals, alloys and polymeric materials [1–3]. Efforts to reduce the use of solvents in the development of products in food, polymer and pharmaceutical industries have been made by using hot-melting procedures [4–7]. Melt kneading methodologies are promising techniques to be used in the near future in pharmaceutical production since they are very valuable from the ecological and quality stand points [8].

Much of this investigation, such as polymorph screening from the melt [9], or identification of organic solid forms [10], requires a deep knowledge of the behaviour of the compounds under investigation during heating/cooling cycles.

Despite its importance, melt quenching is a field still open to investigation, and most the available information comes from metallurgy and polymer chemistry. In contrast, data about medium size organic molecules are relatively scarce.

The present article deals with the growth from the melt of β-adrenergic agents, an important group of drugs used in the treatment of heart diseases. The compounds studied are atenolol, pindolol and betaxolol hydrochloride (Fig. 1).

These have, in common, the 2-isopropylaminoetanol group, and differ each other in the size and polarity of the remaining molecular moieties. Since the three compounds under investigation were in their racemic form, any reference to chirality has been dropped. The methods used in this research were differential scanning calorimetry (DSC) and polarized light thermal microscopy (PLTM).

The patterns of solidification provide information about the structure of the compounds in both liquid and solid states, and also acts as guides to the understanding of the crystallization processes.

Materials and methods

The compounds used in the present study are of the best quality commercially available. All of them had a stated

The coauthors would like to dedicate this manuscript to the memory of Professor M. Luísa P. Leitão for her invaluable contribution to the advance of thermal analysis in their research center.

M. T. S. Rosado · S. C. C. Nunes · M. S. C. Cruz · J. S. Redinha (✉)
Department of Chemistry, University of Coimbra, Rua Larga, 3004-535 Coimbra, Portugal
e-mail: jsredinha@netcabo.pt

J. Canotilho · R. A. E. Castro
Faculty of Pharmacy, University of Coimbra, Rua do Norte, 3000-295 Coimbra, Portugal

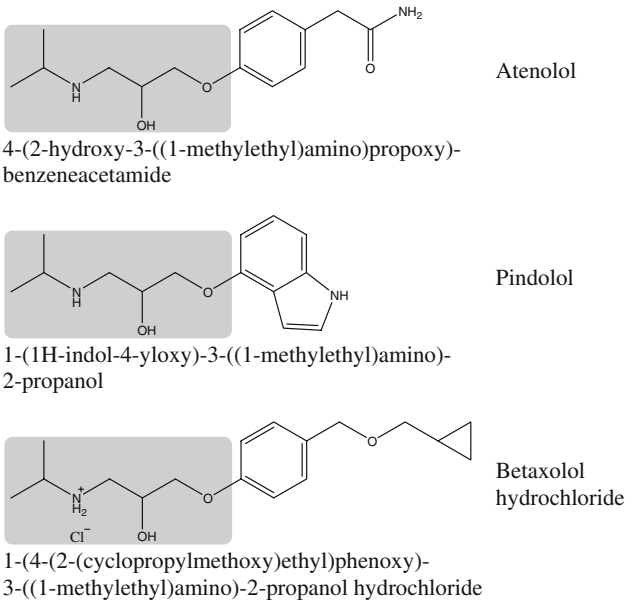

Fig. 1 Structural formula of the β-blockers under study

degree of purity better than 99 mol%, which was confirmed by HPLC.

DSC curves were traced with a Perkin Elmer Pyris 1 calorimeter. Details on the experimental procedure can be found in the authors' previous publications [9]. Special attention was paid to the cell assembling of the atenolol [10] and pindolol [8] because both are oxidised in the liquid state. In the case of atenolol, the degradation process was studied [10]. In the liquid state the amide group is converted into imine giving rise to a dimeric structure, which in turn starts a degradation process. Likewise, indol is converted by oxygen into 3-hidroxy-indol and subsequently into indigo [11, 12]. Since the structural alterations in both compounds are favoured by oxygen the pan containing the samples were assembled inside a glove box under nitrogen atmosphere.

The PLTM equipment consists of a DSC 600 hot/cold stage from Linkam, which allows heating/cooling runs between −160 and 600 °C at rates from 0.1 to 130 °C/min. The liquid nitrogen flux around the cell acts as the cooling agent. The central part of the optical observation instrumentation is a Leica DMRB microscope. A video camera CCD-IRIS/RGB adapted to the microscope sends the image to a DVD recorder or to a computer.

A small amount of the sample under study was introduced into a glass cell in such a way that small aggregates were spread over the bottom. Upon fusion, these aggregates give rise to liquid droplets and their thermal behaviour can then followed during the cooling run. In order to get further information on the phase formed upon cooling a sequent heating run was undertaken on the sample. The scans were performed under a nitrogen atmosphere.

The average linear velocity of crystallization front was determined by recording the position of the solid/liquid interface as a function of the time.

Results

Atenolol

A typical curve on cooling the melt is represented in Fig. 2. A crystallization peak at the temperature of 146 °C is the only thermal signal detected in the temperature range from −160 to 160 °C. The subsequent heating profile is also included. Fusion is the only transition exhibited by atenolol during the heating process. Table 1 shows the temperature and the enthalpy characterizing the phase transformations observed for atenolol in a cooling/heating thermal cycle.

Due to its structural significance, we should stress, from right now, the relevance of the small difference found for the temperature and enthalpy between the crystallization and fusion processes.

The crystal growth from molten atenolol was also accompanied by PLTM at scanning rates from 10 to 50 °C min^{-1}. On cooling, as the temperature reaches approximately 147 °C, the crystalline phase forms a point inside the liquid droplets and suddenly spreads over the drops. The crystallization time lasts <0.04 s. Figure 3 shows the liquid/solid transition for atenolol upon cooling.

(*R*,*S*)-Pindolol

The DSC experiments show that the crystallization of pindolol occurs at 143–132 and/or 75–68 °C according to the cooling rate program. At 10 °C min^{-1} the frequency of the crystallization at the higher temperature range is about 7% and at the lower temperature range is 92%. At a cooling rate of 2 °C min^{-1} the crystallization also occurs at two

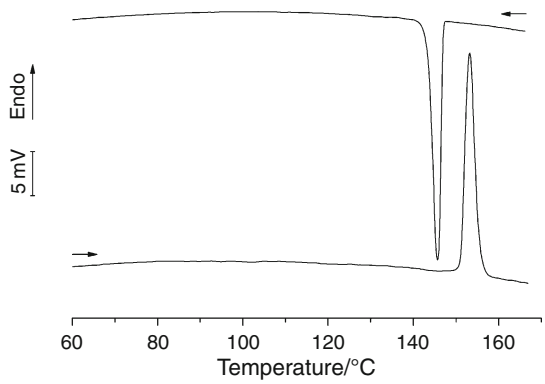

Fig. 2 DSC curves corresponding to the crystallization and fusion of atenolol. Scanning rates, 10 °C min^{-1}

Table 1 Temperature and enthalpy of crystallization and fusion of atenolol determined by DSC at 10 °C min^{-1}

Cooling run			Heating run		
T_{onset}/°C	T_{max}/°C	$-\Delta_{cryst}H$/kJ mol^{-1}	T_{onset}/°C	T_{max}/°C	$\Delta_{fus}H$/kJ mol^{-1}
147.1 ± 1.2	146.5 ± 1.1	36.3 ± 0.7	152.4 ± 0.5	154.7 ± 0.4	36.5 ± 1.1

Mass (2.11 ± 0.3) mg, $n = 20$

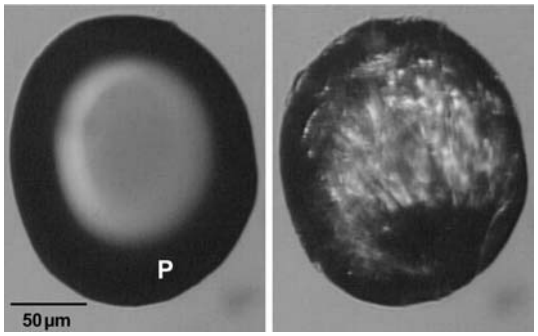

Fig. 3 Starting from P, the crystallization spreads instantaneously over the liquid

temperatures ranges, both of which are higher than those observed for a scanning rate of 10 °C min^{-1}. The decrease of the cooling rate increases the probability of crystallization at the higher temperature range although this remains less frequent than that at the lower temperature. Crystallization outside of the temperature intervals specified above or crystallization at the higher and lower temperature both occurring in the same drop are rare events. The DSC curve patterns corresponding to the thermal cycles run on the pindolol are summarized in Fig. 4 and the relevant values in Table 2.

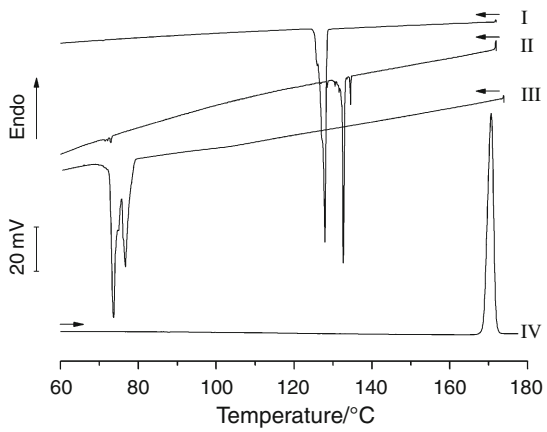

Fig. 4 Cooling and heating DSC curves of pindolol traced at 10 °C min^{-1}: I, crystallization at higher temperature; II, crystallization of most of the sample at higher temperature and a small fraction at lower temperature; III, crystallization of whole sample at the lower temperature; and IV, curve pattern upon reheating

The comparison of the enthalpy changes for the crystallization leads to the conclusion that the degree of crystallinity of the solid at the higher temperatures is greater than that found at the lower temperature range. However, both solid forms are far from perfect crystalline state which is achieved on heating the solid phase further.

The study of the crystallization of pindolol was also undertaken by PLTM. The main features of the phase transition at the higher temperature can be seen in Fig. 5. The nucleation takes place at the surface of the droplet at 137.7 °C, giving rise to a directional growth. The crystallization in the drop proceeds until a sudden stop occurs.

A close examination of the solid/liquid interphases shows that liquid and solid frontiers are a few micrometers apart. As the liquid domain becomes exhausted under crystallization, the growth stop and the border of the neighbouring liquid domain become more pronounced due to the difference of refraction index between the liquid and the surrounding empty space.

A slight motion of the liquid surface, 10 s latter trigger the contact with solid at the point P_1 separated from the liquid by about 5 µm. A secondary crystallization occurs and the solidification process continues (Fig. 5c). Again, a narrower liquid discontinuity is reached and the separated phases are very closely spaced. A slight late crystalline growth at P_2 makes contact with the liquid and the solidification continues.

The variation of the position of the solid/liquid interface as a function of time is depicted in Fig. 7a. The velocity of the crystallization front is about 30 µm s^{-1}. Interruptions of crystal growth in 2–11 and 14–15 s intervals are clearly observed.

The crystallization of pindolol at the lower temperature range is initiated with the formation of one or various nuclei generated inside the droplets exhibiting a radial growth. The solid/liquid interface has a cellular texture and proceeds in a wavelike form (Fig. 6a). A pronounced microsegregation is observed in the crystallization front, giving rise to a blended solid phase (Fig. 6b). Sometimes the growth becomes dendritic in the last stage of the crystallization (Fig. 6c).

The progress of the solid boundary as a function of time following the direction indicated by the arrow is shown in Fig. 7b. In order to obtain a more detailed picture of the instability of the crystal/liquid interface the velocity of the

Table 2 Temperature and enthalpy corresponding to the crystallization and subsequent fusion of pindolol

Scanning rate/°C min^{-1}	Frequency	Cooling run		Heating run	
		T_{onset}/°C	$-\Delta_{cryst}H$/kJ mol^{-1}	T_{onset}/°C	$\Delta_{fus}H$/kJ mol^{-1}
10	3	132 ± 5	47 ± 1	170 ± 1	57 ± 2
	38	67.5 ± 0.8	29.1 ± 0.8		
2	21	143 ± 7	50 ± 3		
	47	75 ± 1	30 ± 1		
1	10			169.7 ± 0.3	58 ± 2

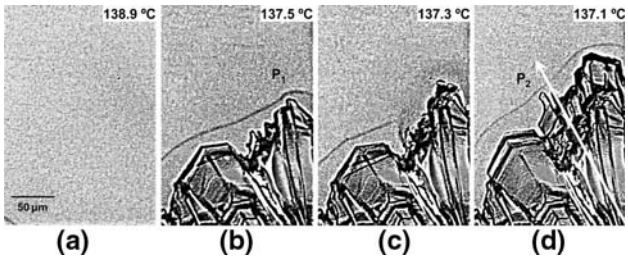

Fig. 5 Micrograph of crystal growth of pindolol from melt. **a** Liquid phase, **b** first stop of the crystallization front, **c** crystallization is reinitiated at P_1 and **d** second stop of the crystallization front. The *arrow* indicate the direction of the velocity measurements. Cooling rate: 2 °C min^{-1}

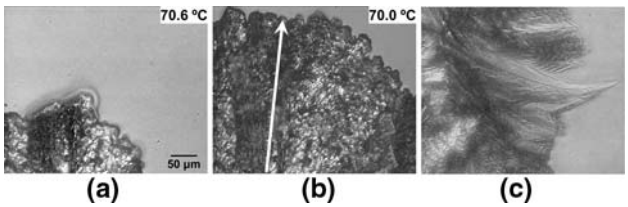

Fig. 6 Microscopic observations of the pindolol crystallization. **a** Snapshot of the crystallization in progress showing the dynamics of the solid/liquid interface, **b** texture of the solid and **c** dendritic texture

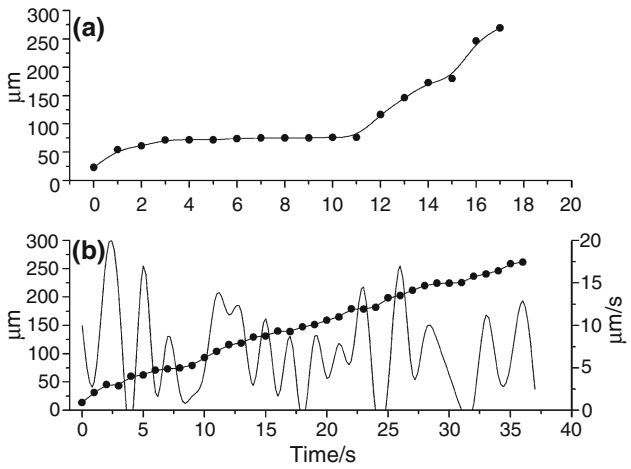

Fig. 7 **a** Growth interface for the crystallization of pindolol at the higher temperature range. Variation of the position of the solid/liquid interface as a function of time. Scanning rate 2 °C min^{-1}. **b** Growth interface for the crystallization of pindolol at the higher temperature range. Variation of the position of the solid/liquid interface as function of time and velocity of the crystallization front at every second (readings on the right hand side scale). Scanning rate: 2 °C min^{-1}

crystallization front versus time is also represented in the same figure. The pattern of the solid/liquid boundary for the crystallization of pindolol at the lower temperature involves a waveform curve characterized by average values for period and amplitude of 2.6 s and 6 µm s^{-1}, respectively.

Betaxolol hydrochloride

Betaxolol hydrochloride is the form under which this β-adrenergic is commonly given as medicine. For this reason, the study was performed on this salt instead on the base form. DSC curves on this compound run from 130 to −160 °C at rates between 2 and 25 °C min^{-1} do not reveal any crystallization peak. A glass transition is observed at temperature around −14 °C and a few thermal signals characterized by an instantaneous heat capacity variation localized in the range −75 to −100 °C are also exhibited (Fig. 8).

Apart from this glass transition the sequent heating run, evidence a small variation of the heat capacity (about 0.03 kJ^{-1} mol^{-1} $°C^{-1}$), around −142 °C and a few exothermic peaks from 25 °C forwards to fusion. Details of the glass transitions of betaxolol hydrochloride on heating can be seen in Fig. 8b, c. The highest value for the enthalpy of crystallization was reached upon cooling the melt at 2 °C min^{-1}, then leaving the sample for 1 h at 25 °C and heating till 130 °C. Under such conditions, the crystallization took place at 53.1 °C accompanied by an enthalpy variation of 21.3 kJ mol^{-1}, even so, a value much smaller compared with that obtained for fusion (32.7 kJ mol^{-1}).

The PLTM observations provide valuable information on the phase transitions undergone by betaxolol hydrochloride during the thermal cycle. On cooling the melt vitrifies at the temperatures referred above and upon further cooling, the glass becomes brittle and a glass cracking is

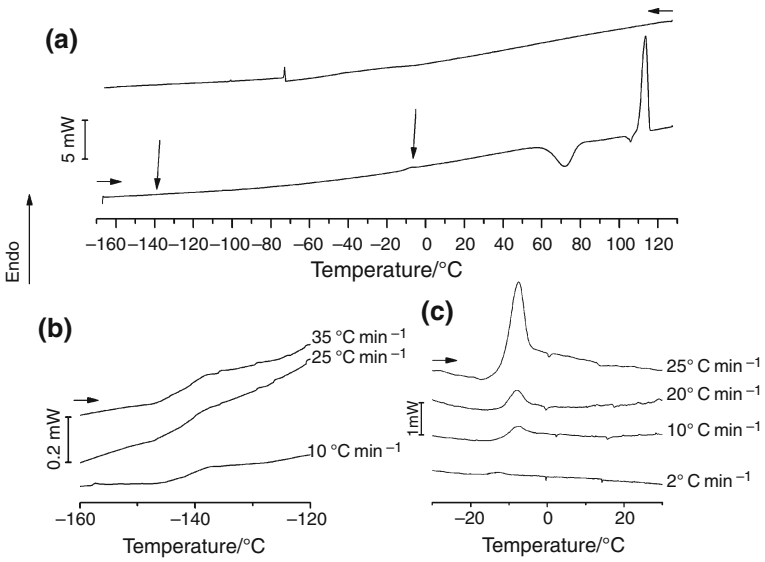

Fig. 8 **a** DSC pattern of a thermal cycle performed on betaxolol hydrochloride at 10 °C min^{-1}. **b**, **c** Details of the glass transitions on the heating run at different scanning rates

observed at temperatures between −70 and −100 °C. The phenomenon is initiated with the fracture of the glass across the whole microscopic observation field, with the decrease of the temperature accompanied by cracking growth out from the original fracture splintering into smaller and smaller sized pieces. As the temperature decreases the glass edges become round and concentric ring bands are observed (Fig. 9).

On heating at any heating rate the crystallization occurs under spherulitic textures (Fig. 10). The formation of the fine-rayed spherulites is followed by liquid rejection, which leads to subsequent solidification. The two solid forms give rise to two liquid phases which are only miscible at temperatures above 130 °C. This means that one upper critical solution temperature is found in the liquid betaxolol hydrochloride at a temperature approximately 20 °C above the melting point.

An overview concerning the experimental observations

The diversity of thermal behaviour manifested by the systems under study gives valuable information about the structure of the compounds and about the crystallization of melts. We now present a brief survey focusing upon the most significant features found for the compound under study.

The low supercooling and the high degree of crystallinity of atenolol obtained from the melt are rather

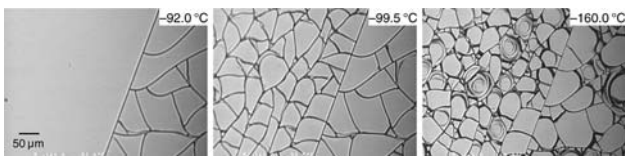

Fig. 9 Optical micrographs of the glass cracking

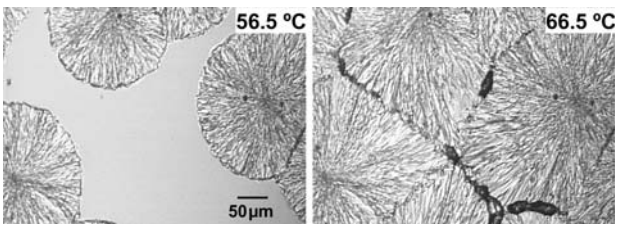

Fig. 10 Optical micrographs of spherulites formed on cold crystallization of betaxolol hydrochloride. The liquid rejected on the crystallization accommodates in the borderline of the spherulites giving a poorly ordered material by solidification

surprising observations. It should be noted that the supercooling given for several simple organic compounds varies from 40 to 120 °C [13]. Thus, the supercooling expected for a compound with flexible backbone, such as atenolol, should be much greater than that observed. The crystallinity perfection of the yield from the melt for organic compounds is usually much lower than that obtained for atenolol. In fact, the degree of crystallinity of atenolol estimated by the ratio between the enthalpy of crystallization and the enthalpy of fusion [14] is 0.994.

Liquid phase decomposition, such as that occurring in pindolol, is a quite common phenomenon in multicomponent polymer systems [15–17]. Liquid–liquid demixing has also been observed in a few single-component inorganic systems [18–22]. Although pindolol is a one-component system, we should bear in mind the fact that like gas [23] and solid forms [8], the molecules in liquid phases can be present in several conformational forms. A preferential interaction between certain types of conformers can provide enough microheterogeneity to make it capable of phase separation in the supercooled melt.

The interplay between liquid–liquid demixing and other phase transitions, in particular crystallization, is still poorly

understood. In pindolol this phenomenon is so closely related with crystallization that one is a consequence of the other. This behaviour confirms the recent interpretation of Hu et al. [17] that liquid demixing is driven by a selective crystallizability of one of the components. The proximity of the values for the temperature of crystallization and liquid–liquid demixing means that the processes take place at a temperature close to the critical point. Indeed, the metastable zone between the binodal and the spinodal curves becomes increasingly narrower as the critical point is approached [24].

Although a previous liquid separation does not occur in the solidification of the pindolol at the lower temperature, liquid incompatibility is manifested by microsegregation.

Betaxolol hydrochloride is a glass-forming compound on cooling the melt. A partial crystallization takes place on heating giving rise to two liquid phases by fusion. The upper critical solution temperature is observed at about 130 °C.

From the molecules to the crystal

The present investigation deals with three different molecules having in common the isopropylamino-2-propanol group, which contains functional groups capable of forming hydrogen bonds. Meanwhile they exhibit quite different crystallization ability from even the simplest medium, the melt. The interpretation of the data obtained for these systems is of great importance because, first they provide deep insights into the structure of the compounds in question in both solid and liquid states, second, they contribute to clarify important pathways of the crystallization from the melt and third, they point out the big challenge of crystal structure prediction from the features of the molecule.

The supramolecular structure resulting from molecular self-assembly by progressive cooling of the melt depends, among other factors, on the nature and strength of the intermolecular forces, the flexibility of the molecular chain and the structure of the melt.

Provided that hydrogen bonds are present in most organic crystals and considering their characteristics (relative strength, directionality and selectivity), these can be considered as fundamental design elements in crystalline architecture [25]. The hydrogen bond network in the crystalline form of the three β-adrenergic are presented in Table 3.

In atenolol the intermolecular interaction involve NH_2 (amide), CO and OH groups [26, 27]. Besides these three moderate strength hydrogen bonds given in Table 3, a weak intermolecular CH$\cdots\pi$ bond can also contribute to the structure. The molecules are linked together leaving short molecular fragments between them. The only molecular fragment with free internal rotation is the terminal isopropyl group. Such a structural pattern formed practically in thermodynamical equilibrium conditions favours the formation of a very high crystallinity phase.

Table 3 Geometric parameters of D–H···A and enthalpies of hydrogen bonds for atenolol [26, 27], pindolol [30, 31] and betaxolol hydrochloride [28, 32]

Hydrogen bond D–H···A	H···A/Å[a]	D–H···A/°[a]	ΔH/kJ mol^{-1}[b]
Atenolol			
O–H···N_{amine}	2.49	119.7	17
N_{amide}–H···O=C (*i*)	2.04	173.9	20
N_{amide}–H···O=C (*ii*)	2.06	161.5	20
Pindolol			
N_{amine}–H···O_{ether}	2.98	106	Weak
O–H···N_{amine}	1.78	172	25
N_{indol}–H···O–H	2.03	156	12
N_{amine}–H···O–H (intra)	2.31	114	5
Betaxolol hydrochloride			
N^+–H_2···Cl^- (*i*)	2.16	177.2	31
N^+–H_2···Cl^- (*ii*)	2.45	160.5	5
O–H···Cl^- (*i*)	2.08	166.0	25

[a] Single crystal X-ray diffraction data

[b] Calculated from stretching vibration red shift

The structural features of pindolol molecule with respect to intermolecular hydrogen bonding and molecular flexibility is rather similar to that of atenolol. Thus, it would be expected that solidification takes place leading to a crystalline form. However, the lower degree of crystallinity as compared with that of atenolol is due to the more complex structure of the melt. The high crystallization barrier (high supercooling) and the liquid immiscibility are strong indications of the complex mechanism of the crystallization process.

Finally, betaxolol hydrochloride on cooling the melt is an excellent glass-forming system. This is an expected behaviour from the crystal structure [28, 29]. In fact the ammonium and the hydroxyl groups of the same molecule are hydrogen bonded to a chloride ion through an intermolecular bridge. No other specific bonds exist along the fully extended backbone whose conformational flexibility gives rise to a disordered structure.

Conclusions

The combination of DSC and PLTM techniques provides unique information on main pathways of crystallization processes. Evidence and interpretation are given of

liquid–liquid demixing in the supercooled melt of an organic homomolecular system; the structural interpretation based on the crystallization front texture and velocity; the relationship between the crystallization process and the supramolecular structure of the solids are particularly relevant points in the present work.

References

1. Turi A. Thermal characterization of polymorphic materials. London: Academic Press; 1981.
2. Mullin JW. Crystallization. Oxford: Elsevier; 2001.
3. Ropp RC. Solid state chemistry. Amsterdam: Elsevier; 2003.
4. Kim JW, Ulrich J. Prediction of degree of deformation and crystallization time of molten droplets in pastillation process. Int J Pharm. 2003;257:205–15.
5. Goskonda SR, Hileman GA, Upadrashta SM. Development of matrix controlled release beads by extrusion-spheronization technology using a statistical screening design. Drug Dev Ind Pharm. 1994;20:279–92.
6. Schaefer T, Holm P, Kristensen HG. Melt granulation in a laboratory scale high shear mixer. Drug Dev Ind Pharm. 1990;16: 1249–77.
7. Passerini N, Albertini B, González-Rodríguez ML, Cavallari C, Rodriguez L. Preparation and characterisation of ibuprofen–poloxamer 188 granules obtained by melt granulation. Eur J Pharm Sci. 2002;15:71–8.
8. Nunes SCC, Eusebio ME, Leitão MLP, Redinha JS. Polymorphism of pindolol, 1-(1H-indol-4-yloxyl)-3-isopropylamino-propan-2-ol. Int J Pharm. 2004;285:13–21.
9. Canotilho J, Costa FS, Sousa AT, Redinha JS, Leitão MLP. Melting curves of terfenadine crystallized from different solvents. J Therm Anal Calorim. 1998;54:139–49.
10. Castro RAE. Antagonistas Adrenérgicos Selectivos beta 1: Estrutura do Atenolol. Ph.D. thesis, Universidade de Coimbra; 2006.
11. Mahrous MS, Issa AS, Ahmed NS. Oxidants for the colorimetric determination of pindolol. Talanta. 1992;39:69–72.
12. Stenlake JB. Foundations of molecular pharmacology, vol. 1. London: The Athlone Press of the University of London; 1979.
13. Kelton KF. Crystal nucleation in liquid and glasses in solid state physics. London: Academic Press; 1991.
14. Montserrat S, Roman F, Colomer P. Study of the crystallization and melting region of PET and PEN and their blends by TMDSC. J Therm Anal Calorim. 2003;72:657–66.
15. Balsara NP, Fetters LJ, Hadjichristidis N, Lohse DJ, Han CC, Graessley WW, et al. Thermodynamic interactions in model polyolefin blends obtained by small-angle neutron scattering. Macromolecules. 1992;25:6137–47.
16. Briber RM, Khoury F. The morphology of poly(vinylidene fluoride) crystallized from blends of poly(vinylidene fluoride) and poly(ethyl acrylate). J Polym Sci B. 1993;31:1253–72.
17. Hu WB, Mathot VBF. Liquid–liquid demixing in a binary polymer blend driven solely by the component-selective crystallizability. J Chem Phys. 2003;119:10953–8.
18. Katayama Y, Mizutani T, Utsumi W, Shimomura O, Yamakata M, Funakoshi K. A first-order liquid–liquid phase transition in phosphorus. Nature. 2000;403:170–3.
19. Mishima O. Liquid–liquid critical point in heavy water. Phys Rev Lett. 2000;85:334–6.
20. Soper AK, Ricci MA. Structures of high-density and low-density water. Phys Rev Lett. 2000;84:2881–4.
21. Lacks DJ. First-order amorphous–amorphous transformation in silica. Phys Rev Lett. 2000;84:4629–32.
22. Vanthiel M, Ree FH. High-pressure liquid–liquid phase change in carbon. Phys Rev B. 1993;48:3591–9.
23. Nunes SCC, Jesus AJL, Rosado MTS, Eusebio MES. Conformational study of isolated pindolol by HF, DFT and MP2 calculations. J Mol Struct (Theochem). 2007;806:231–8.
24. Debenedetti PG. Metastable liquids: concepts and principles. Princeton: Princeton University Press; 1996.
25. Desiraju GR. Supramolecular synthons in crystal engineering—a new organic synthesis. Angew Chem Int Ed Eng. 1995;34:2311–27.
26. Castro RAE, Canotilho J, Barbosa RM, Silva MR, Beja AM, Paixa JA, et al. Conformational isomorphism of organic crystals: racemic and homochiral Atenolol. Cryst Growth Des. 2007;7: 496–500.
27. Castro RAE, Canotilho J, Barbosa RM, Redinha JS. Infrared spectroscopy of racemic and enantiomeric forms of atenolol. Spectrochim Acta A. 2007;67:1194–200.
28. Canotilho J, Castro RAE, Teixeira MHSF, Leitão MLP, Redinha JS. Infrared study of the acidic and basic forms of betaxolol. Spectrochim Acta A. 2006;64:279–86.
29. Canotilho J, Castro RAE, Rosado MTS, Ramos Silva M, Matos Beja A, Paixão JA, et al. The structure of betaxolol from single crystal X-ray diffraction and natural bond orbital analysis. J Mol Struct. 2008;891:437–42.
30. Chattopadhyay TK, Palmer RA, Mahadevan D. Molecular and absolute crystal structure of pindolol-1-(1H-indol-4-yloxy)-3-[(1-methylethyl)amino]-2-propanol: a specific beta-adrenoreceptor antagonist with partial agonist activity. J Chem Crystallogr. 1995;25:195–9.
31. Castro RAE, Canotilho J, Nunes SCC, Eusebio ME, Redinha JS. A study of the structure of the pindolol based on infrared spectroscopy and natural bond orbital theory. Spectrochim Acta A. 2009;72:819–26.
32. Mairesse G, Boivin JC, Thomas DJ, Bonte JP, Lesieur D, Lespagnol C. Structure du chlorhydrate de l'[hydroxy-1-(R, S) isopropylamino-2 éthyl]-6 dihydro-2, 3 benzoxazole-1, 3 one-2, $C_{12}H_{16}N_2O_3$•HCl. Acta Crystallogr C. 1984;40:1432–4.